The Borea project: a quadrotor uav cradle-to-grave design for space gnc prototyping and testing

IAC-18-F1.2.3

The Borea project: a quadrotor UAV cradle-to-grave design for space GNC prototyping and testing

Luigi Colangelo[a]*, Carlos Perez-Montenegro[a], Mauricio A. Lotufo[b], Carlo Novara[a]

[a] *Department of Electronics and Telecommunications, Politecnico di Torino, Corso Duca degli Abruzzi, 24, 10129 Torino*, luigi.colangelo@polito.it
[b] *Modelway s.r.l., Torino*
* Corresponding Author

Abstract

Unmanned Aerial Vehicles (UAVs) and, more specifically, n-copters have come to prominence in the last decade due to their several applications. Also, in the automatic control research community UAVs have drawn great attention, since their non-linear and under-actuated nature making them suitable for testing a wide range of control architectures and algorithms. In this paper, prominent theoretical aspects, simulations, and experimental results of the Borea project are presented. The Borea project aims at testing space guidance, navigation, and control (GNC) algorithms leveraging a simplified, rapidly prototypable, low-cost, and easy-to-test quadrotor platform. More precisely, one of the main project objectives consists in testing Moon and Mars planetary landing algorithms, thanks to the similitude, in the command authority and the landing approach, between n-copters and spacecraft; during the propulsive landing phase. Indeed, both n-copters and spacecraft can provide a thrust vector characterized by constant direction and adjustable magnitude. This similitude approach makes it possible to anticipate issues and avoid failures such as those that occurred in the Schiaparelli Mars Lander. To this aim, the complete control unit design, and the UAV plant electro-mechanical prototyping were addressed; so far. Specifically, the control unit was designed within the framework of the Embedded Model Control (EMC) methodology. The EMC design, based on an internal model, also includes the uncertainties as disturbances to be estimated and actively rejected. The Borea UAV has been endowed with a control system leveraging a wide range of automatic control concepts, ranging from modelling, identification, and linear and non-linear control laws, to deal with its position, velocity, and attitude regulation. To sum up, all these results were achieved by means of a properly structured cradle-to-grave design process which, starting from the simultaneous plant modelling and prototyping, ended up with a complete flight tests campaign. Most notably, the testing process involved intensive numerical simulations as well as multi-stage hardware/plant tests and models validation. From the control perspective, the several developed controllers were tuned and tested, via proper simulations and on-purpose flight tests, aiming at validating, from time to time, specific functionalities and control performances. Finally, some results coming from high-fidelity simulations, the hardware and model testing, and in-flight operations are provided to underline the most relevant aspects of the Borea plant and the control unit performance.

Keywords: Unmanned Aerial Vehicle (UAV), Guidance, Navigation, Control, Model-based Control

Nomenclature

This section is not numbered. A nomenclature section could be provided when there are mathematical symbols in your paper. Superscripts and subscripts must be listed separately. Nomenclature definitions should not appear again in the text.

Acronyms/Abbreviations

This section is not numbered. Define acronyms and abbreviations that are not standard in this section. Such acronyms and abbreviations that are unavoidable in the abstract must be defined at their first mention there. Ensure consistency of abbreviations throughout the article. Always use the full title followed by the acronym (abbreviation) to be used, e.g., reusable suborbital launch vehicle (RSLV), International Space Station (ISS).

1. Introduction

In the last few years, unmanned aerial vehicles (UAVs) have been proposed more and more in a wide range of applications, ranging from defence to civilian purposes (e.g. reconnaissance, borders patrolling, traffic monitoring, search and rescue) [1]. Among the several UAV configurations, rotary-wing vehicles come to prominence over fixed-wing aircraft; due to their distinctive features, like the ability to hover, as well as the possibility of vertical take-off and landing (VTOL vehicles).

Among rotary-wing UAVs, quadrotors show an interesting set of valuable traits with respect to other UAVs [2], such as an extended manoeuvrability, yet a rapidly prototypable, low-cost, and easy-to-test platform. Hence, quadrotors have received much attention both from the application perspective, and in

the UAV research community. From this perspective, researchers have been focusing on a wide range of topics, often linked to the quadrotor nonlinear behaviour and under-actuated behaviour, spanning from autonomy to path planning and sensor fusion.

In the control literature, the problem of the quadrotor UAV attitude and displacement control has been faced with both linear and nonlinear techniques. As a matter of fact, PID controllers, as in [3] and [4], are the most common linear control approach. Conversely, most of the non-linear control solutions mainly propose to address the quadrotor control either via Sliding Model Control (SMC) laws, back-stepping, and feedback linearization (FL). Improved SMC solutions have been presented, for instance, in [5] and [6], with a high-order SMC and an adaptive version, respectively. In addition, [7] showed how the sliding variables are driven to zero also in the presence of bounded uncertainties and disturbances, with a sliding mode disturbance observer. Back-stepping techniques for the quadrotor attitude stabilization have been presented in [8], in presence of external torque disturbance, and in [9], in combination with the H_∞ results. Finally, [5] leverage the feedback linearization technique, coupled with a high-order sliding mode observer, by considering an extended model composed by the quadrotor model plus additional states to linearize the extended model with a static non-linear feedback. Conversely, an adaptive version of the sliding mode control was proposed in [6] to overcome the well-known FL weaknesses.

However, the above-mentioned approaches may show limitations due to their difficulty in dealing with the significant disturbances, model uncertainties, and non-linearities which typically affect UAV quadrotors operations. For example, the FL approach may result quite sensitive to external disturbances and sensor noises because of the high order derivatives involved in it. When relevant disturbances or uncertainties occur, the control performance may get significantly worse, possibly causing unstable behaviours. One way to deal with this sort of problems is by means of a disturbance-rejection-based control methodology [11, 12]. Indeed, feedback controllers can become more robust against model uncertainties and disturbances if they are estimated and rejected in real-time. In control literature, the disturbance rejection problem is a lively research area, and several interesting approaches have been proposed as the Active Disturbance Rejection Control (ADRC) [10], disturbance observer-based control [13], or extended high-gain observer-based control [14], and Embedded Model Control (EMC) [12].

This latter approach adopted in this study, as per Subsec. 1.1, calls for a hierarchical and multi-rate control unit around the real-time internal model of the UAV input-output controllable dynamics, also called Embedded Model. Most notably, this quadrotor Embedded Model includes a simple but effective disturbance estimation dynamics. Such disturbance dynamics allows, inter alia, to adopt a simplified LTI (controllable) internal model, while directly rejecting the perturbations from the LTI model via the control law.

1.1 The Borea Quadrotor UAV

The discovery of space remains one of the great sources of knowledge and support for many research projects, yet what happened with Schiaparelli Mars lander shows that there are still great challenges in planetary landing that must be overcome. Planetary landing integrates many technologies, many of which can be emulated with low cost with n-copters. N-copters have kinematics, dynamics, and command authority comparable to spacecraft in their propulsive landing phase: a thrust vector characterized by constant direction and adjustable magnitude, by means of pitch and roll manoeuvres. Hence, n-copter UAVs may be employed to design and test spacecraft landing algorithms, thus making possible to foresee and counteract potential issues and to avoid failures.

To this aim, the Borea project, within the Politecnico di Torino, aimed to design, prototype, build, and test a quadrotor to test space Guidance, Navigation and Control (GNC) algorithms [15].

One of the most challenging segment of the Borea cradle-to-grave project was undoubtedly the control unit. Indeed, the Borea quadrotor (see Fig. 1) has been endowed with a complete control system in order to control its position, velocity, and attitude [16]. From this perspective, a complex mix of linear and non-linear control design techniques were adopted [17]; starting from the feedback linearization technique, which was applied to the non-linear quadrotor model. In turn, the feedback-linearized input-output model of the UAV quadrotor, collecting all the non-linearities at the command level, powered the Embedded Model Control design, pursuing the estimation and the rejection of a wide range of disturbances affecting the quadrotor in-flight. To this purpose, the feedback linearized model was completed by suitable predictors of the quadrotor attitude and displacement state variables, as well as stochastic disturbance observers [ref].

From the sensor perspective, the Borea quadrotor has been equipped with a wide range of sensors: three MEMS gyroscope and accelerometers, magnetometers, a barometric altimeter, a sonar and a GPS receiver. Consequently, a full set of calibration procedures was devised and successfully tested. To sum up, the devised sensor network is equivalent to the sensors embarked on a lander spacecraft, although a GPS receiver was used in the first tests, and with limited performance.

In parallel to the hardware developments, and following an architecture of a space mission, a

Matlab/Simulink high-fidelity simulator has been also developed to support the control design, and a safe testing before the experimental flight trials.

To sum up, the designed EMC control unit was also benchmarked against state-of-the-art high-performance UAV controllers [18] as well as extensively tested with: (i) a high-fidelity simulator [16,17], (ii) a laboratory experimental test-bench [19], and (iii) in-flight [ref].

The remainder of this paper is organised as follows. Section 2 focuses on the Borea UAV platform, summarizing the main aspects of the electro-mechanical prototype. In Section 3, the Borea control unit is described, reviewing its building blocks according to the EMC design methodology. The experimental results of the EMC attitude controller are depicted in Section 4, after a discussion about the calibration procedures established to ensure the consistency of the Borea sensors setup. To conclude, Section 5 draws the conclusions and sketches out potential future research directions.

2. The Electro-Mechanical Platform of Borea

In this section, the main aspects of the Borea UAV are presented. The main topic treated here is the electro-mechanical prototype, at first. Then, the major design choices in terms of sensors and actuators are outlined.

2.2 The Platform: Borea electro-mechanical prototype

The Borea is a four rotor UAV (see Fig. 1) which was designed and developed bearing in mind the objective of testing spacecraft landing algorithms, by leveraging their analogy with rotating wings UAVs, such as quadrotors. As a by-product, the complete control unit fulfilling our primary purpose, lead to investigate the applicability of disturbance-rejection-based control methodologies, in non-linear and under-actuated systems affected by uncertainties and external disturbances.

The structure of the Borea prototype, made mainly by wood, comprises three major parts (cf. Fig. 1): (i) a main frame for motors, ESC, and landing feet, (ii) a battery support, and (iii) a board electronics support plate. Interestingly, properly-sized rubber dampers, at the connection points between the main frame and the electronic plate, are used to abate the micro-vibrations induced by the actuators chain. The whole structure is characterized by an arm-length of 0.25 m, a total weight around 2.0 kg, and an almost diagonal inertia matrix, i.e. $J = \text{diag}\{0.032, 0.032, 0.061\}$ kgm. It is worth to notice, the four rotors nominally lay on the same plane and cannot tilt. In short, each propeller has a fixed pitch and it is driven by a dedicated DC brushless motor and controlled by its own power driver (namely, the Electronic Speed Controller or ESC), as per Fig. 1.

The Borea UAV control unit, also in charge to read sensors' data and to provide real-rime commands, is based on a Sparkfun UDB5 board (see Fig. 2) that includes the Inertial Measurement Unit (IMU) MPU-6000 and a 16-bit micro-controller. Specifically, the micro-controller, belonging to the dsPIC33F series manufactured by Microchip, has a fixed-point arithmetic unit. In turn, the IMU is made up by tri-axial MEMS gyroscopes and accelerometers. For the sake of completeness, the flight controller board and its electrical inter-connections to the several UAV subsystems are depicted in Fig. 1.4. The flight control board is also able to receive the operator's commands, via radio-link. Such a communication with the ground station, also accounting for the telemetry and health data transmission (e.g. battery voltage), is performed by means of proper Radio Frequency (RF) modules, called "X-Bee" and manufactured by DIGI 1 (cf. Fig. 3). As a matter of fact, being bi-directional, thus allowing both the transmission and the reception, two X-Bee modules enabled a reliable wireless communication between Borea and the ground station, without any risk of mutual interference or detrimental communication errors. From this perspective, flight raw data are also recorded and stored, in a binary format, through micro SD-card. As a matter of fact, the analysis of flight data was proven to be crucial for the tuning of the control algorithms as well as for the test and development iterations of the Borea prototype.

Finally, electrical power is supplied to the system by a Lithium Polymer battery (LiPo) of 12.6 V, in full charge condition (11.1 V nominal voltage). In the current configuration, the battery capacity of 5 Ah guarantees 8 minutes of cruise flight-time, approximately (a 30% of residual charge is mandatory in order to preserve the battery integrity). This in-flight endurance was deemed sufficient to test the planetary landing, which usually has a limited maneuver time.

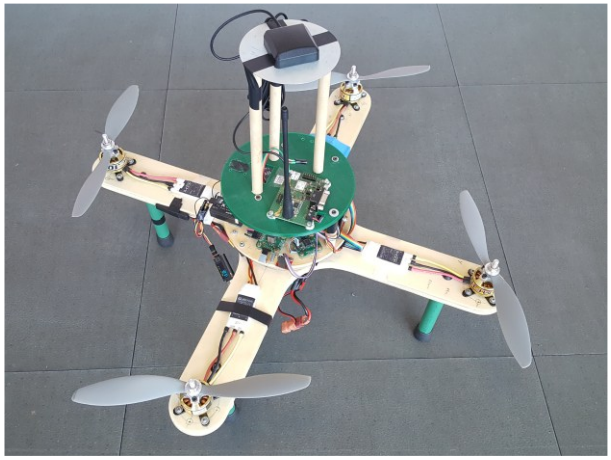

Fig. 1. The Borea quadrotor UAV platform

1.2 Sensors and Actuators Configuration

The Borea quadrotor platform is endowed with several sensors either integrated within the Sparkfun UDB5 main board (as per Fig. 2), or on-purpose procured, connected to the board itself, and properly configured. In short, the main board provides the UAV with a complete set of inertial navigation functions, being equipped with gyroscopes and accelerometers to suitably derive the quadrotor attitude and position. In addition, an external magnetometer sensor was added in order to measure the Earth magnetic field and to perform full attitude estimation via sensor fusion algorithms. Finally, a sonar and a differential GPS receiver were mounted on-board, to retrieve a finer measure of the quadrotor position.

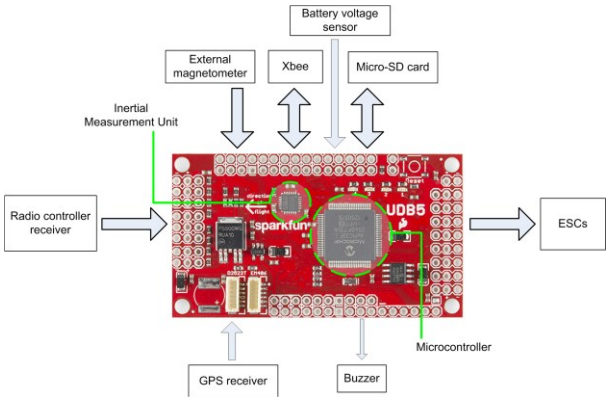

Fig. 2. The Borea quadrotor UAV platform: detail of the flight controller board and its subsystems connections.

The Borea project was based on low-cost components, of the COTS type. For this reason, integrated MEMS inertial sensors were considered; although characterized by a small form factor and a sufficient level of accuracy for the mission objectives. Similarly, the employed three-axial magnetometer, able to measure direction and intensity of the magnetic field, is the Honeywell HMC5883L; based on the Anisotropic Magneto-resistive technology. Concerning the precise positioning measurement, the U-blox C94-M8P application board, integrating the NEO-M8P-2 module, was chosen as GNSS instrument. Specifically, this GNSS kit includes two RF antennas, two GPS active antennas, and two configurable boards: one configured as base station (fixed position during the flight), the other one (the rover board) embarked on the quadrotor. Interestingly, the chosen NEO-M8P module can perform Real Time Kinematics (RTK) positioning when correction messages arrive from the base station. Generally speaking, GNSS instruments with RTK capability are more and more adopted in UAV applications, due to their high-performance level at a reasonably low-cost. An RTK-enabled GNSS instrument is able to provide measurements with an accuracy up to the centimetre level. In shirt, the RTK technique is based on the estimate of the distance between the UAV and the ground station receivers; based on the GNSS carrier phase measurements, instead of using the pseudo-code measurements only, as in the classical DGPS. In turn, the smaller noise in carrier measurements let the position error in RTK to reach levels far littler than the pseudo-range case.

To conclude, a wide range of sensor modelling, and experimental tests were conducted in order to improve the quadrotor simulator fidelity and to sustain the control design process. In particular, calibration algorithms and procedure, both on-line and off-line, were devised in order to compensate the significant errors potentially affecting the control performance.

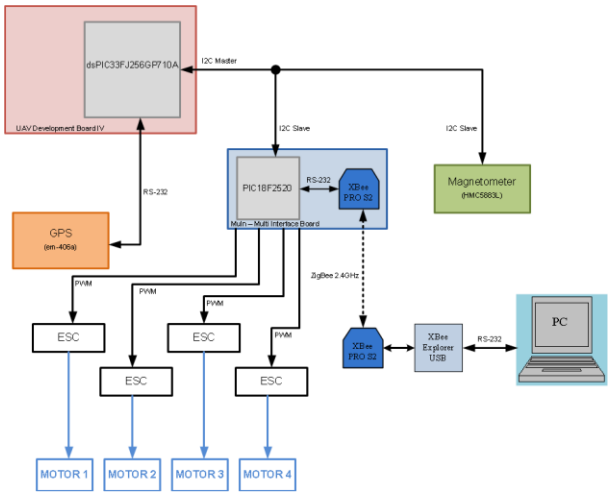

Fig. 3. The Borea quadrotor UAV: flight controller board functional architecture

The quadrotor actuator system can be ideally decomposed into three main components (Fig. 4): (i) the electric motors, (ii) the propellers, rigidly jointed to the motors, and (iii) the power driver, aiming at regulating the motors angular rate according to the reference set by the controller command (namely, the Electronic Speed Controller, or ESC). From the functional perspective, the main flight control board is connected with the ESCs of the four motors, to transmit the control command signals via the Pulse Width Modulation (PWM) output; at 400 Hz (cf. Fig. 3).

The actuator is a dynamic system whose main input is the propeller angular rate reference, while the main output is the propeller thrust (Fig. 4). As a matter of fact, such a system has a non-linear behaviour, making its control a quite challenging task. This results to be especially true when complex manoeuvres must be executed, with high precision.

Consequently, to enhance the performance of the model-based control unit, the input-output model of the Borea UAV actuator was identified [19], to be explicitly included into the controller model [17]. To this aim, a

two-step identification procedure was performed, whose rationale was the separation of the static part of the input-output relationship from the dynamic one (see also Fig. 4). The identification revealed a low-frequency dynamic behaviour, which was proven to be a fundamental shaping factor for the controller design. What is more, from the identified model, it was also possible to infer how the employed commercial ESCs have dependencies from the battery voltage. Therefore, to deal with this issue, the battery voltage v_b was considered as input of the actuator (see Fig. 4).

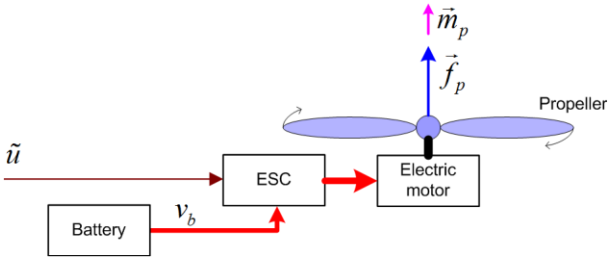

Fig. 4. The Borea quadrotor UAV: actuator system functional architecture

To sum up, the actuator model was identified from sets of data collected in a wide range of experimental tests, performed on a single actuator (under the reasonable assumption that all the actuators would behave similarly). Then, the actuator model was built by considering a typical Hammerstein-Wiener structure: a dynamic linear time invariant (LTI) system placed between two static non-linear blocks, viz:

$$\begin{aligned} z(t) &= g(\tilde{\quad} \quad v_{b\max} - v_b(t)), \\ \dot{\quad} &\quad \omega_p(t) + pz(t), \\ f_p(t) &= f(\omega_p(t)), \\ m_p(t) &= h(\omega_p(t)). \end{aligned} \tag{1}$$

The identification process was based on the two subsystems, defined by the first two equations in (1), defining the Hammerstein system, namely a cascaded connection of a static non-linearity and a dynamic LTI block. Notably, this model structure was validated by the experimental data.

3. Model-based Control Unit

In this section, the control design methodology, namely the Embedded Model Control (EMC), is briefly outlined and then the main parts of the control unit, designed for the Borea UAV, are reviewed; in line with Fig. 5.

3.1 The Embedded Model Control: a Disturbance-rejection-based Approach

The control unit was designed via the EMC methodology [12]. The EMC is a model-based control methodology based on two main pillars (Fig. 5): (i) the embedded model, and the (ii) disturbance rejection. The embedded model (cf. Fig. 5) is a simplified input-output representation of the plant to be controlled, whose design is performed in a systematic way starting from the plant detailed model and the control requirements. Embedded model includes the plant input-output dynamics controllable by the command, and the disturbance dynamics module, describing the disturbance class affecting the model output and to be rejected.

To the purpose of the disturbance rejection, the disturbance dynamics is synthesized as a parameter-free cascade of discrete-time integrators driven by an unpredictable input, here referred as noises ($\overline{\mathbf{w}}$ in Fig. 5). This allows to represent a generic class of signals, able to reproduce the large class of disturbances, parametric uncertainties and neglected dynamics potentially affecting the controllable part of the simplified input-output model (controllable dynamics, in Fig. 5).

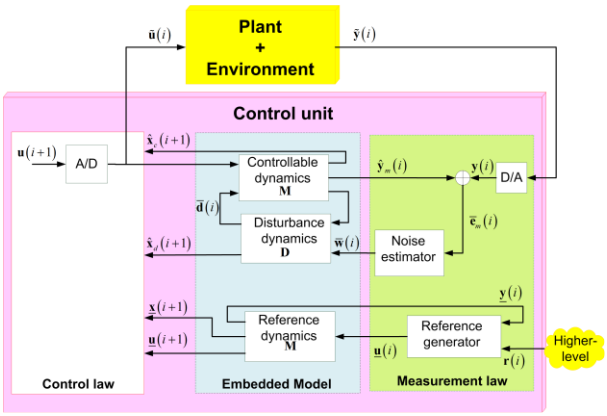

Fig. 5. The Embedded Model Control unit

In turn, the Noise Estimator (NE, Fig. 5) is in charge of estimating the input noises, and this provides the output-to-state feedback closing the loop. Indeed, the loop defined by the EM plus the NE represents a state predictor, computing the one-step predictions of the controllable and disturbance states.

In short, the noise estimator leverages the model error ($\overline{\mathbf{e}}_m$ in Fig. 5), i.e.:

$$\overline{\mathbf{e}}_m(i) = \mathbf{y}(i) - \hat{\mathbf{y}}_m(i), \tag{2}$$

which is function of neglected dynamics and sensor noise, being the difference between the measure $\mathbf{y}$ and the model output $\hat{\mathbf{y}}_m$, to obtain a viable feedback source for the noise estimation. On the other side, being crucial

for the final performance, the NE design must ensure the best trade-off between stability and disturbance estimation. From this perspective, a systematic procedure for controller design was addressed in [12], in general, and in [17], for the Borea case. Nevertheless, the eigenvalue tuning was refined by means of numerical simulations and in-field tests (cf. the final values in Table 1).

Finally, as per Fig. 5, the closed-loop predictor model and disturbance states are employed both for the control law synthesis, and to build the structure of the reference generator. The reference generator is based on the controllable dynamics and interface the control unit with the external operator to provide the reference states and command to the control law.

3.2 The Borea Model

In this section, the modelling of the Borea quadrotor is sketched. To this aim, given a generic angle α, s_α and c_α refer to the functions sin(α) and cos(α), respectively. Further, the α Euler elementary attitude rotations are represented by the matrices X(α), Y(α), and Z(α).

Hence, starting from the UAV attitude model, let us consider an attitude kinematics represented through the Euler angles: roll φ, pitch θ, and yaw ψ. Thus, the quadrotor attitude can be described by the 1-2-3 body to fixed rotation:

$$R_{bi}(\varphi,\theta,\psi) = \begin{bmatrix} c_\theta c_\psi & -c_\theta s_\psi & s_\theta \\ s_\varphi s_\theta c_\psi + c_\varphi s_\psi & -s_\varphi s_\theta s_\psi + c_\varphi c_\psi & -s_\varphi c_\theta \\ -c_\varphi s_\theta c_\psi & c_\varphi s_\theta s_\psi + s_\varphi c_\psi & c_\varphi c_\theta \end{bmatrix}. \tag{3}$$

Then, being $\boldsymbol{\theta}(t)$ the Euler angles state vector, the attitude kinematics can be derived, in a straightforward way:

$$\dot{\boldsymbol{\theta}}(t) = \mathrm{A}(\boldsymbol{\theta}(t))\boldsymbol{\omega}(t), \quad \boldsymbol{\theta}(0) = \boldsymbol{\theta}_0,$$
$$\mathrm{A}(\boldsymbol{\theta}(t)) = \frac{1}{c_\theta}\begin{bmatrix} c_\psi & -s_\psi & 0 \\ c_\theta s_\psi & c_\theta c_\psi & 0 \\ -s_\theta c_\psi & s_\theta s_\psi & c \end{bmatrix}, \tag{4}$$

being $\boldsymbol{\omega}(t)$ the angular rate vector, in body frame coordinates.

The UAV attitude model is completed by the attitude dynamics. To this aim, introducing the angular acceleration $\mathbf{u}(t)$, the system is described as:

$$\dot{\boldsymbol{\omega}}(t) = J^{-1}\boldsymbol{\omega}(t) \times J\boldsymbol{\omega}(t) + \mathbf{d}(t), \quad \boldsymbol{\omega}(0) = \boldsymbol{\omega}_0 \tag{5}$$

where $\mathbf{d}(t)$ stands for the unknown disturbances, to be estimated and rejected.

The dynamic model of the UAV Center of Mass (CoM) displacement was defined in the inertial reference frame. Thus, by considering the 3D CoM position $\mathbf{r}(t)$ as the model output, it holds:

$$\dot{\mathbf{r}}(t) = \mathbf{v}(t), \quad \mathbf{r}(0) = \mathbf{r}_0,$$
$$\dot{\mathbf{v}}(t) = R_{bi}(t)\begin{bmatrix} 0 \\ 0 \\ u_1(t) \end{bmatrix} - \mathbf{g} - \mathbf{a}_d(t), \quad \mathbf{v}(0) = \mathbf{v}_0,$$
$$\mathbf{y}(t) = \mathbf{r}(t) \tag{6}$$

where, $\mathbf{g}$ is the gravity vector, $\mathbf{a}_d(t)$ gathers all the external disturbances. Therefore, the complete model have a state vector $\mathbf{x}(t) = \begin{bmatrix}\mathbf{r} & \mathbf{v} & \boldsymbol{\theta} & \boldsymbol{\omega}\end{bmatrix}^T$ collecting the 12 state variables describing the Borea inertial position and velocity, as well as its three attitude angles and angular rates.

3.3 The State Predictor

The UAV model defined in 3.2 is the basis for the Embedded Model in the control unit. Indeed, the first step for the design of the attitude and the CoM displacement state predictors the derivations of the respective EMs: discrete time models, composed by a simplified input-output dynamics controllable by the command, plus a disturbance dynamics, acting on the controllable part. The state predictor allows a reliable estimation of both the controllable and the disturbance states, to be cancelled by means of the control law.

For the sake of brevity, in the following the paper is focused on the analysis to the UAV attitude state predictor derivation. A short summary of the UAV CoM displacement control design principle is outlined in Subsec. 3.5, and deepened in [17].

In order to obtain the EM, a Euler forward discretization was applied to the attitude model in (4) and (5); with a control time unit of 20 ms. The attitude controller was based on three separated single axis EMs, to reduce the design complexity. According to this perspective, the main coupling effects due to the neglected attitude kinematics were considered as (partially unknown) disturbances, to be estimated. The resulting DT EM holds:

$$\begin{bmatrix} \hat{\mathbf{x}}_c \\ \hat{\mathbf{x}}_d \end{bmatrix}(i+1) = \begin{bmatrix} A_c & H_c \\ \mathbf{0} & A_d \end{bmatrix}\begin{bmatrix} \hat{\mathbf{x}}_c \\ \hat{\mathbf{x}}_d \end{bmatrix}(i) + \begin{bmatrix} B_c \\ 0 \end{bmatrix}u(i) + \begin{bmatrix} G_c \\ G_d \end{bmatrix}\overline{\mathbf{w}}(i),$$
$$\hat{y}_m = \begin{bmatrix} C_c & C_d \end{bmatrix}\begin{bmatrix} \hat{\mathbf{x}}_c \\ \hat{\mathbf{x}}_d \end{bmatrix}(i), \tag{7}$$

Where $\hat{\mathbf{x}}_c$ is the controllable state vector (attitude angle, rate, and actuator dynamics), $\hat{\mathbf{x}}_d$ is the disturbance dynamics state vector, and:

$$A_c = \begin{bmatrix} 1 & 1 & 0 \\ 0 & 1 & 1 \\ 0 & 0 & 1-\beta \end{bmatrix}, B_c = \begin{bmatrix} 0 \\ 0 \\ \beta \end{bmatrix}, A_d = \begin{bmatrix} 1 & 1 \\ 0 & 1 \end{bmatrix},$$

$$H_c = \begin{bmatrix} 0 & 0 \\ 1 & 0 \\ 0 & 0 \end{bmatrix}, G_c = \begin{bmatrix} 0 & 0 & 0 & 0 \\ 0 & 1 & 0 & 0 \\ \beta & 0 & 0 & 0 \end{bmatrix}, G_d = \begin{bmatrix} 0 & 0 \\ 0 & 0 \\ 1 & 0 \\ 0 & 1 \end{bmatrix}^T. \quad (8)$$

In (8), the controllable and the disturbance sub-systems are shaped by the matrices A_c and A_d, respectively. From (8), the closed-loop state equation of the state predictor is obtained via the NE, which is determined by four static gains, i.e.:

$$\overline{\mathbf{w}}(\mathrm{i}) = \begin{bmatrix} l_0 & l_1 & l_2 & l_3 \end{bmatrix}^T \overline{\mathbf{e}}_m, \quad (9)$$

being $\overline{\mathbf{e}}_m$, the model error above defined. To conclude, the design and computation of the NE gains, pursuing the closed-loop stabilisation of the state predictor, is straightforward after fixing the desired set of closed-loop eigenvalues in (8); through pole placement.

3.4 The Control Law

The model and disturbance states, computed via the state predictor, drive the control law. Within the EMC framework, the control law (Fig. 5) consists in a full state feedback, with a disturbance rejection term. Hence, the predicted controllable states are leveraged in the feedback signal, while the disturbance states shape the disturbance rejection capability of the control law. Thus, the command signal $\mathbf{u}(\mathrm{i})$ holds:

$$\mathbf{u}(\mathrm{i}) = \underline{\mathbf{u}}(\mathrm{i}) + K\mathbf{e}_c(\mathrm{i}) - \mathrm{M}\,\hat{\mathbf{x}}_d, \quad \text{where } \mathbf{e}_c(\mathrm{i}) = \underline{\mathbf{x}}_c(\mathrm{i}) - \hat{\mathbf{x}}_c(\mathrm{i}) - Q\hat{\mathbf{x}}_d(\mathrm{i}). \quad (10)$$

In (10), the nominal command $\underline{\mathbf{u}}(\mathrm{i})$ is the feed-forward component of the command, while the tracking error $\mathbf{e}_c(\mathrm{i})$ defines the full state feedback component, whose component are designed to stabilize the closed-loop state matrix (cf. control law feedback, in Table 1). Finally, the EMC disturbance rejection considers the effect of disturbances not entering the model at the command level, through the matrix Q.

3.5 The CoM Position Controller

The Borea UAV control unit also envisages full CoM displacement regulation and tracking. To this aim, in the Borea project, we investigated the use of the Feedback Linearization (FL) approach. As a matter of fact, FL has been proved to be a powerful control technique to be applied to non-linear systems. What is more, FL technique allows to collect all the model non-linearities at the command level, thus allowing to achieve input-output linearization, via feedback, in case of cancellation of non-linearities. Nevertheless, since those non-linear terms are somehow uncertain, a way to strengthen control robustness consists in treating model uncertain non-linearities as unknown disturbances. To this aim, FL was deemed as suitably fitting the EMC modelling structure, including a disturbance estimation and rejection capabilities. Hence, this technique was applied to the Borea quadrotor model introduced in 3.2, as an innovative tool for the EM model design.

4. Experimental Results

In this section, results about the experiments carried out to develop and test the Borea control unit are presented. Interestingly, the attitude control tests consisted in both high-fidelity simulations, and UAV flight trials. For the sake of completeness, Table 1 lists the values of the main parameters characterizing the control unit and the Borea experimental setup.

Table 1. Borea UAV: platform and control unit experimental parameters.

Parameter	Value	Unit	Note
Mass	2.5	kg	Nominal
Inter-axial length	0.5	m	Nominal
Inertia matrix	diag{0.30; 0.31; 0.65}	kg·m^2	Nominal
Control step	0.020	s	
Simulation step	0.0005	s	
Complementary eig.	**Value**	**Order**	**Note**
Predictor (position)	0.01	Order 4	f_r = 0.08 Hz
Predictor (attitude - tilt)	0.01	Order 2	f_q = 0.08 Hz
Predictor (acceleration)	0.2	Order 2	f_a = 1.60 Hz
Control law feedback	0.2	Order 4	$f_{\min}$ = 0.8 Hz

4.1 Sensor Calibration

The calibration of the sensors embarked on the Borea platform was the aim of the first set of simulation and flight tests. To this aim, although classical procedures overcome the sensor systematic errors via on-line sensor calibration, our solution aimed to avoid this additional step before starting the automatic mission

phase. Hence, the proposed solution, consistently with the space control, envisaged two flight control modes: (i) calibration mode, (ii) mission mode. In turn, the calibration mode involves both the gyroscope and the accelerometer. First of all, a gyroscope on-ground calibration takes charge of the gyroscope bias, which is easily identified in a no-motion condition. Secondly, after the take-off, a hovering manoeuvre is performed to allow the accelerometer calibration [ref]. At this proposal, Fig. 6 depicts the time profile of the accelerometer measure, throughout a typical flight mission profile. It is worth to observe the two flight control modes: calibration and mission. Specifically, the accelerometer bias is automatically detected and cancelled in about 1 s. After then, the control unit switches to the mission mode, in which the accelerometer loop and the attitude loop can be closed with the calibrated accelerometer measurement.

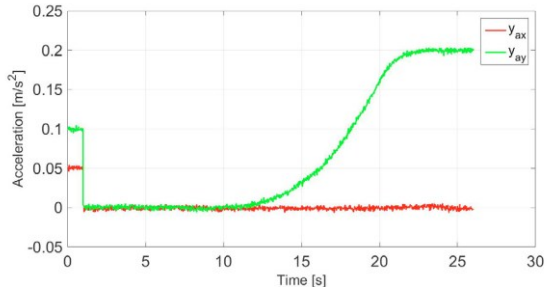

Fig. 6. Sensors calibration: accelerometer measurement

4.2 Simulation Results and Flight Tests

The designed attitude and CoM displacement controllers were validated through a wide simulation campaign. To this purpose, one pillar of the Borea project was a high-fidelity simulator which was developed by the research group. The Borea simulator is implemented in Matlab/Simulink and includes all quadrotor dynamics and kinematics as well as the sensor and actuators models. Furthermore, the simulator includes the major aspects of the outdoor flight environment, like drag, wind, and terrain models. In addition, a configuration script allows one to choose among the several control laws and loop schemes available in the control unit, as well as the controller configuration (e.g. the eigenvalues tuning) and the simulation environment (e.g. drag, wind).

For the results concerning the attitude showed below, an angular sequence test-trajectory was defined to test the controller performance: a positive plus a negative pitch movement, followed by a hovering phase, and then a positive heading rotation.

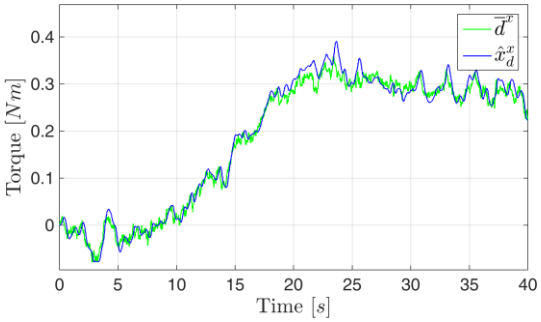

Fig. 7. Attitude control - simulated test: disturbance estimation

Figure 7 focuses on one of the leading aspects of an EMC control unit. Indeed, it shows the simulated comparison between a real unknown disturbance, affecting the UAV, and the disturbance estimated by the designed disturbance dynamics, within the Borea control unit. It is interesting to notice how the estimated attitude disturbance signal, $\hat{\mathbf{x}}_d$ in (7), is able to reliably match the true one, up to a significant bandwidth.

The real flight test campaign of the attitude controller was performed in two stages. First of all, a laboratory mono-axial experimental test-bench, designed on purpose, allowed a safe control tuning and the test of the angular guidance algorithms. Secondly, open-air flight trials were carried out to validate the UAV take-off, hovering and landing phases, before testing different attitude manoeuvres and configurations.

In Fig. 8, it is depicted the outcome of a horizontal outdoor flight trial, at moderate velocity, to test the tracking angle performance of the controller. Specifically, Fig. 8 plots the tilt tracking errors (i.e. reference minus estimate). From the analysis of the trends, there is evidence to indicate that the estimated attitude angles, $\hat{\mathbf{x}}_c$ in (7), effectively follow the attitude reference provided by the guidance algorithm; even in presence of disturbance and kinematics couplings.

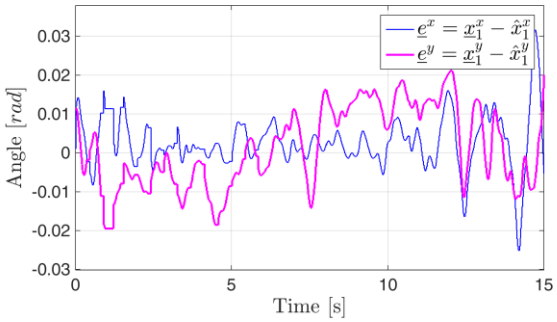

Fig. 8. Attitude control - flight test: tilt angles tracking errors

For the sake of completeness, also results from the CoM displacement control are presented and discussed.

The test starts with 40 s of hovering flight, followed by a quadrotor 4 m CoM displacement, along the Y-axis, while keeping constant the vertical and X-axis positions. In addition, external torque disturbances affect the UAV motion, as a nearly-constant horizontal wind (8m/s) and an artificial torque effect (initial ramp ending in a constant trend at 0.15 mNm), on the X-axis. Finally, a polynomial guidance algorithm was set up to provide the quadrotor with proper references to be tracked by the controllable state variables.

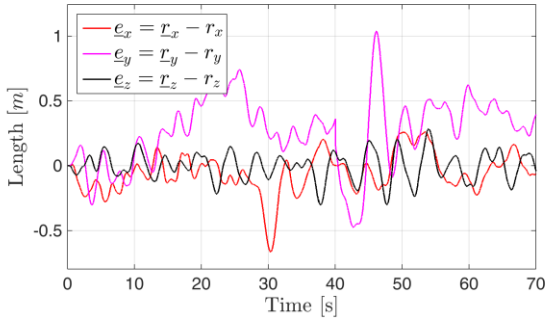

Fig. 9. Displacement control - simulated test: CoM position tracking error

Figure 9 depicts the simulated position tracking error, computed as the difference between the reference to be followed and the plant measurement output. Therefore, it includes also modelling errors as well as sensors errors and noises. The error behaviour in Fig. 9 suggests a good capability of the control law to track the position reference, with a positioning error peak roughly about 1 m; in module. The order of magnitude of this value was deemed in line with the low-cost COTS level of hardware leveraged for the Borea UAV platform, yet satisfying the expected performance requirements in terms of tracking precision and external disturbance rejection.

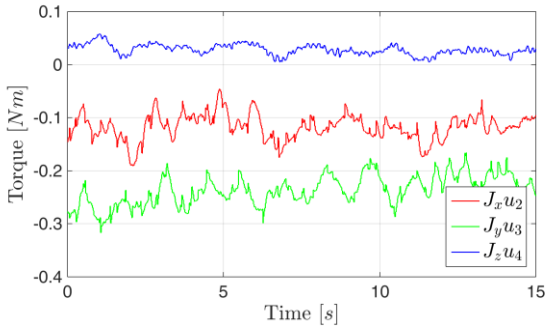

Fig. 10. Displacement control - flight test: command torques

To conclude, Fig. 10 depicts the typical command torques characterizing the Borea CoM displacement controller, in real outdoor flight. As above stated, both X and Y-axes were affected by a (nearly constant) disturbance torques; likely due to actuators unbalancing, any sort of mechanical vibrations, and external ambient factors (e.g. wind). The controller exerts an additional torque to ensure a stable tilted condition, during the UAV horizontal displacement. Also, in this case, the displayed values are deemed coherent with the hardware requirements and capabilities, as well as safely below the UAV actuators saturation thresholds; as expected and pursued by the design.

5. Conclusions

In this paper, a complete overview of the main aspects of the Borea project, and its status, is provided; including, simulations, and experimental results. The Borea project aims at creating an autonomous UAV quadrotor platform for the space GNC algorithms development and testing.

In this study, the Embedded Model Control (EMC) methodology was successfully applied for the Borea control unit design. The Embedded Model Control is a model-based control technique, allowing the estimation and rejection of a wide range of disturbances affecting the quadrotor in flight.

First of all, the UAV attitude reconstruction and control were pursued, in order to make the quadrotor able to fly in outdoor environments. Hence, the feedback linearization technique was applied to the non-linear quadrotor model, since its structure is enhanced by the EMC capability to estimate as disturbances the model non-linearities, and then reject them.

In parallel with the control unit, also a complete electro-mechanical prototype was designed, built, and tested. Attention was devoted to the sensors and actuators selection, test, and calibration, as a way to ensure an adequate level of flight and manoeuvre performance, though employing low-cost and COTS hardware.

Further, a multi-stage tests procedure was implemented in which the plant performance and the designed control unit were preliminary tested and fine-tuned via a high-fidelity simulator. Then, an experimental tests campaign was carried out, via a laboratory test-bench, at first, and then in full outdoor flight.

The finding indicates that the EMC control unit, based on the feedback linearized model, works properly and allows the quadrotor to follow the desired flight trajectory, in a wide set of outdoor flight conditions. On the other side, the attitude controller ensures a proper attitude regulation, plus a compelling capability to withstand external disturbances and uncertain kinematics couplings.

Future work should both evaluate, by simulation and test, the impact of potential UAV plant upgrades on the control unit performance level and emulate autonomous tests of planetary landing.

References

[1] K. P. Valavanis, G. J. Vachtsevanos. Handbook of unmanned aerial vehicles. Springer Publishing Company, Incorporated, 2014.

[2] S. Gupte, P. I. T. Mohandas, and J. M. Conrad. A survey of quadrotor unmanned aerial vehicles. In Southeastcon, 2012 Proceedings of IEEE, pages 1–6. IEEE, 2012.

[3] K. H. Ang, G. Chong, and Y. Li. PID control system analysis, design, and technology. IEEE transactions on control systems technology, 13(4):559–576, 2005.

[4] A. Tayebi and S. McGilvray. Attitude stabilization of a VTOL quadrotor aircraft. IEEE Transactions on control systems technology, 14(3):562–571, 2006.

[5] A. Benallegue, A. Mokhtari, and L. Fridman. Feedback Linearization and High Order Sliding Mode Observer for a Quadrotor UAV. In Variable Structure Systems, 2006. VSS'06. International Workshop on, pages 365–372. IEEE, 2006.

[6] D. Lee, H. J. Kim, H. Jin Kim, and S. Sastry. Feedback linearization vs. adaptive sliding mode control for a quadrotor helicopter. International Journal of Control, Automation and Systems, 7(3):419–428, May 2009.

[7] L. Besnard, Y. B. Shtessel, and B. Landrum. Quadrotor vehicle control via sliding mode controller driven by sliding mode disturbance observer. Journal of the Franklin Institute, 349(2):658–684, 2012.

[8] X. Huo, M. Huo, and H. Reza Karimi. Attitude stabilization control of a quadrotor UAV by using backstepping approach. Mathematical Problems in Engineering, 2014, 2014.

[9] K. Djamel, M. Abdellah, and A. Benallegue. Attitude optimal backstepping controller based for a UAV. Mathematical Problems in Engineering, 2016, 2016.

[10] J. Han, From PID to active disturbance rejection control, IEEE Transactions 500 on Industrial Electronics 56 (3) (2009) 900-906.

[11] E. Canuto, C. P. Montenegro, L. Colangelo, and M. A. Lotufo. Active disturbance rejection control and embedded model control: a case study comparison. In Control Conference (CCC) 33rd Chinese (pp. 3697-3702). IEEE, 2014

[12] E. Canuto, C. P. Montenegro, L. Colangelo, and M. A. Lotufo. Embedded model control: Design separation under uncertainty. In Control Conference (CCC) 33rd Chinese (pp. 3637-3643). IEEE, 2014

[13] M. Nakao, K. Ohnishi, K. Miyachi, A robust decentralized joint control based on interference estimation, in: Proceedings. 1987 IEEE International Conference on Robotics and Automation, Vol. 4, 1987, pp. 326-331.

[14] L. B. Freidovich, H. K. Khalil, Performance recovery of feedback linearization-based designs, IEEE Transactions on Automatic Control 53 (10) (2008) 2324-2334.

[15] E. Canuto, and C. Perez-Montenegro. Modelling and control of a small quadrotor for testing propulsive planetary landing guidance, navigation and control. In International Astronautical Congress: IAC Proceedings (p. A3). International Astronautical Federation, 2012.

[16] C. Perez-Montenegro, M. A. Lotufo, E. Canuto. Control architecture and simulation of the borea quadrotor. IFAC Proceedings Vol. 2, 168-73, 2013

[17] M. A. Lotufo, L. Colangelo, C. Perez-Montenegro, Canuto E. The feedback linearisation method for Embedded Model Control: The Borea project case-study. In Control and Automation (MED) 23th Mediterranean Conference on 2015 Jun 16 (pp. 501-507). IEEE, 2015

[18] G. Farid, M. Hongwei, S. M. Ali, and Q. A. Liwei. A review on linear and nonlinear control techniques for position and attitude control of a quadrotor. Control and Intelligent Systems, 45(1), 2017.

[19] M. A. Lotufo, C. Perez-Montenegro, L. Colangelo, E. Canuto, and C. Novara. Identification and control of a quadrotor from experimental data. In Control and Automation (MED) 24th Mediterranean Conference on 2016 Jun 21 (pp. 895-900). IEEE, 2016.